

**Article Type:** Full Paper

## **Mechanisms of atmospheric pressure plasma treatment of BOPP**

David A. G. Sawtell\*, Zaenab Abd-Allah, James W. Bradley, Glen T. West, Peter J. Kelly

---

Dr D. A. G. Sawtell, Dr Z. Abd-Allah, Dr G. T. West, Prof. P. J. Kelly  
Faculty of Science and Engineering, Manchester Metropolitan University, M1 5GD, UK.  
[d.sawtell@mmu.ac.uk](mailto:d.sawtell@mmu.ac.uk)  
Prof. J. W. Bradley  
Department of Electrical Engineering and Electronics, University of Liverpool, L69 3GJ, UK.

---

### **Abstract**

Surface energy increase of polymers with plasma treatment is an industrially significant process. The mechanisms behind this process are little understood, with work addressing the water contact angle decrease with treatment and changes in surface chemistry. Work presented here addresses the mechanism of this surface energy increase, by using crystalline biaxially orientated polypropylene (BOPP) films to identify plasma induced structural changes. Increased crystallinity of the BOPP films were observed by ATR-FTIR spectroscopy, indicating preferential oxidation of amorphous regions of the BOPP films by the plasma. This crystal structure change correlates with XRD peak shifts, implying relaxation of crystal regions into regions previously occupied by amorphous BOPP. The trend in surface energy increases also correlates with the effective increase in crystallinity.

### **1 Introduction**

Surface functionalisation of biaxially orientated polypropylene films is of industrial significance due to the added value of improved dye adhesion that such treatments provide. Typically surface functionalisation is carried out through the use of an atmospheric pressure plasma, either corona or dielectric barrier discharge. The aim of such treatments is to increase

the surface energy of the polypropylene film such that it is above that of the surface tension of typical water based inks, maximising adhesion of these inks to the polypropylene surface.<sup>[1]</sup>

The increase in surface energy is generally attributed to an increase of oxygen or nitrogen based functional groups at the surface due to reactions with oxygen or nitrogen species generated within the plasma. Some work has been carried out to elucidate the mechanisms of surface modification of BOPP films by non-thermal atmospheric pressure plasmas, the most extensive being that of Dorai and Kushner<sup>[2]</sup> on air corona treatments of polypropylene. In this case, there tends to be rapid reaction of the polypropylene surface with atomic oxygen and hydroxide radicals generated in the plasma, leaving alcohol or carbonyl functional groups present at the surface. The rate of reaction of atomic nitrogen with polypropylene is also stated to be negligible in comparison with atomic oxygen.<sup>[2]</sup> Increasing concentrations of oxygen also act to limit atomic nitrogen formation in nitrogen plasmas due to preferential formation of NO<sub>x</sub>.<sup>[3]</sup> Recent work by Shaw *et al* highlights a direct link between atomic oxygen formation in helium atmospheric pressure plasma jets and the modification of polypropylene surfaces, in contrast to surface reactions with singlet delta oxygen and ozone.<sup>[4]</sup> Polypropylene undergoes scission of its constituent chains either due to reactions with reactive oxygen species, or due to being subjected to ultraviolet light of particular wavelengths, leaving the polypropylene radicals free to react with oxygen and reactive oxygen species in their proximity.<sup>[5]</sup> These scissions of the polypropylene chains also lead to the formation of low molecular weight oxidised materials (LMWOM), which can cause poor adhesion of inks to the surface.<sup>[6]</sup>

Dielectric barrier discharges allow for treatments of large surface areas,<sup>[7]</sup> which is of great importance for industrial systems. There are indications that dielectric barrier discharges in nitrogen minimise LMWOM formation, compared to standard corona treatments in air.<sup>[8]</sup> The literature suggests that oxygen concentration is key to reducing the formation of LMWOM no

matter the type of plasma, with dielectric barrier discharges in air also exhibiting LMWOM formation.<sup>[9]</sup> This is in contrast to helium and argon based discharges, which do not exhibit the same LMWOM formation.<sup>[10]</sup> Increased formation of atomic oxygen with a significant increase in oxygen concentration is perhaps the reason for increased LMWOM formation with air based plasmas, with the atomic oxygen causing excess scission of the polypropylene chains and hence LMWOM formation.<sup>[2]</sup>

Atmospheric pressure nitrogen plasmas formed in dielectric barrier discharges tend to be filamentary, but under certain conditions can form a uniform Townsend discharge.<sup>[11]</sup> With trace amounts of other gases, the stability criteria for nitrogen plasmas is broken,<sup>[12]</sup> leaving a filamentary discharge. The vast majority of industrial treatments in nitrogen are likely carried out in the filamentary mode, and this does not seem to have any negative impact on the quality of the films treated. Even so, questions do remain over the spatial variation of the treatments, and there have been extremely limited attempts to address this.

We intend to examine the process of nitrogen dielectric barrier discharge surface treatment of BOPP films in depth, analysing the overall mechanism by looking at changes in crystallinity, surface functional groups and surface energy. The variability of the treatment will also be examined considering the potential for filamentary discharges to cause damage to the polymer surface.

## **2 Experimental Part**

### **2.1 Equipment and materials**

A dielectric barrier discharge operating in the filamentary regime is formed from two alumina plates measuring 240 by 50 mm, with 6  $\mu\text{m}$  thick copper coatings measuring 230 by 40 mm sputtered onto the back of the plates acting as electrodes. The dielectrics were spaced 1 mm

apart, with the BOPP film resting on the bottom dielectric which in turn is connected to the grounded electrode. The dielectrics are encased within Perspex, with Perspex also sealing the sides of the reactor. A baffled mixing chamber supplied the gases evenly over the 240 mm width of the dielectric, the exit of the reactor was open to atmosphere. The power supply consists of a signal generator (TTi TG1000), audio amplifier (ProSound 1600) and a custom built high voltage transformer (Amethyst Designs). Current and voltage measurements were made with a Pearson 4100 current monitor and a Tektroniks 1000:1 voltage probe, recorded on a Tektronix DPO 3014 digital oscilloscope. Applied power was calculated from the current and voltage measurements. 99.999 % purity nitrogen (BOC) was introduced at a total flow rate of between 1 and 10 SLM using MKS G Series mass flow controllers, connected a 647C control box. Treatments were carried out over 5 to 60 seconds on 50  $\mu\text{m}$  thick, highly crystalline C50 BOPP film provided by Innovia Films, no significant heating of the BOPP was measured over these treatment times. These films were stored in ambient air prior to plasma treatment. Four replicates at each condition were made.

## **2.2 Surface measurements**

Films were analysed pre and post treatment with a Thermo Nicolet 380 FTIR with a single pass diamond ATR Smart iTR attachment. Each spectra was averaged over 16 scans, with a resolution of 4  $\text{cm}^{-1}$ . Particular interest was paid to the peaks at 997  $\text{cm}^{-1}$ , 973  $\text{cm}^{-1}$  and 840  $\text{cm}^{-1}$ , the ratio of which has been shown to be indicative of the degree of crystallinity of the polypropylene.<sup>[13]</sup> Measurements were made ten times across the width of each 240 by 50 mm sample to account for spatial variation in treatment. Depth of penetration of the infrared beam was estimated to be 1  $\mu\text{m}$  into the surface, using the standard depth of penetration calculation.

A PanAnalytical X'Pert Powder X-ray diffractometer was used to collect the diffraction patterns, enabling the analysis of the effects of plasma treatment on the crystal structure in the

near surface region. Scans were made from 10 to 40  $2\theta$  at a step size of  $0.0002^\circ$ , and diffracted X-rays were collected with a PIXcel detector.

Surface topology changes were assessed using a ZeGage Optical Profilometer. A 50 times objective was used, with a scan range of 50  $\mu\text{m}$  using a rigorous scan. Scans were subsequently corrected for any tilt in the collected results, and a fourier filter was applied to remove any ripples due to the film not lying flat prior to the measurement. Samples were also scanned ten times across the width of the surface. Roughness values are the standard arithmetic average values, typically denoted as  $S_a$ .

Contact angles ( $\theta$ ) of sessile drops of HPLC grade water, ethylene glycol and diiodomethane (Sigma Aldrich) were all measured with a Krüss MobileDrop goniometer. Without the ability to measure advancing and receding contact angles, measurements of ten sessile drops of each liquid type were performed across the width of the samples. The method of Van Oss *et al.*,<sup>[14]</sup> was used for calculating the surface energy ( $\gamma_s$ ) of the films from these measurements, according to the following equation:

$$(1 + \gamma_l) \cos \theta = 2 \left( \sqrt{\gamma_s^{LW} \gamma_l^{LW}} + \sqrt{\gamma_s^A \gamma_l^B} + \sqrt{\gamma_s^B \gamma_l^A} \right) \quad (1)$$

Where the subscripts  $l$  and  $s$  denote the surface energy of the solid and liquid respectively. The superscript  $LW$  denotes the Lifshitz-van der Waals components of the surface energy, and the superscripts  $A$  and  $B$  denote the Lewis acid and Lewis base parameters of the surface energy. The acid and base terms can be combined into the Lewis acid base (superscript  $AB$ ) component of the surface energy:

$$\gamma_l^{AB} = \sqrt{\gamma_l^A \gamma_l^B} \quad (2)$$

and subsequently the overall surface energy can be calculated as the sum of the Lifshitz van der Waals and Lewis acid base components:

$$\gamma_i = \gamma_i^{LW} + \gamma_i^{AB} \quad (3)$$

The components of the surface energy can then be used to assess the hydrophobicity, or Gibbs free energy of attraction between the surface and water (surface energies of which are denoted by subscript w),<sup>[15]</sup> can be calculated by the following:

$$\Delta G_{sw} = -2 \left( \left( \sqrt{\gamma_s^{LW}} - \sqrt{\gamma_w^{LW}} \right)^2 + 2 \left( \sqrt{\gamma_s^a \gamma_s^b} + \sqrt{\gamma_w^a \gamma_w^b} - \sqrt{\gamma_s^a \gamma_w^b} - \sqrt{\gamma_w^a \gamma_s^b} \right) \right) \quad (4)$$

### 3 Results and Discussion

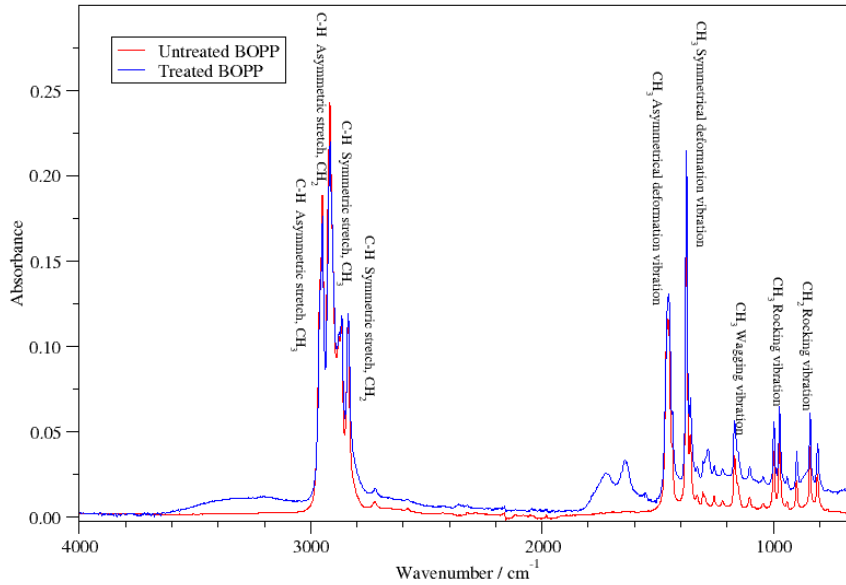


*Figure 1:* ATR-FTIR spectra comparing untreated and treated BOPP film, with band assignments.<sup>[16]</sup> The plasma treatment was at a power of 0.9 W, frequency of 5 kHz and flow rate of 10 slm over a period of 1 minute.

ATR-FTIR spectra for both untreated and treated BOPP films are presented in **Figure 1**, with key band assignments indicated. After plasma treatment, bands in the FTIR spectra start to come up at between 1500 to 1800  $\text{cm}^{-1}$ , as seen in figure 1. This indicates increased functional groups due to either C=O stretches from carbonyl and amide functional groups, or

N-H deformations within secondary amide functional groups. The absorption peaks due to these stretches tend to increase with plasma treatment time, indicating an increase of these particular functional groups on the surface of the polypropylene with increasing exposure time to the plasma. **Figure 2** shows the increase in the intensity of the amide C=O band at  $1660\text{ cm}^{-1}$  with time for different operating flow-rates, frequencies and powers. Figure 2a shows that there is a tendency for the peak to plateau with time, indicating a maximum increase in functionality for a given set of frequencies and powers. Figure 2b demonstrates that higher flow rates of nitrogen produce similar results in terms of amide C=O formation on the surface of the BOPP film, however the reduction in flow causes a greater formation rate of the carbonyl groups. This is due to an increase in the residence time of more oxidising species, and hence the amide groups form at an increased rate.

Upon treatment with atmospheric pressure plasma, the ratios of band positions at  $997\text{ cm}^{-1}$ ,  $973\text{ cm}^{-1}$  and  $840\text{ cm}^{-1}$  shifted in relation to each other, indicative of changes in the crystal structure.<sup>[11]</sup> These ratios were calculated for the spectra produced at the differing powers and flow rates, and these can be seen in **Figure 3**. Both Figure 3a and 3b indicate that there is an overall increase in the crystallinity of the material being measured. The suggestion is that the amorphous regions in between crystalline lamella are being oxidised preferentially due to the porous nature of these regions, whilst only the outer surface of the lamellae are able to react with atomic oxygen formed in the plasma. This effect plateaus out very quickly, perhaps due to the amorphous regions being consumed rapidly, with the outer edges of the lamellae reacting at a slower rate. The electrodes were not active long enough to heat up, both alumina and BOPP are poor conductors of heat, and the nitrogen flow aided convection, therefore any thermal contributions to crystal structure changes are thought to be negligible.

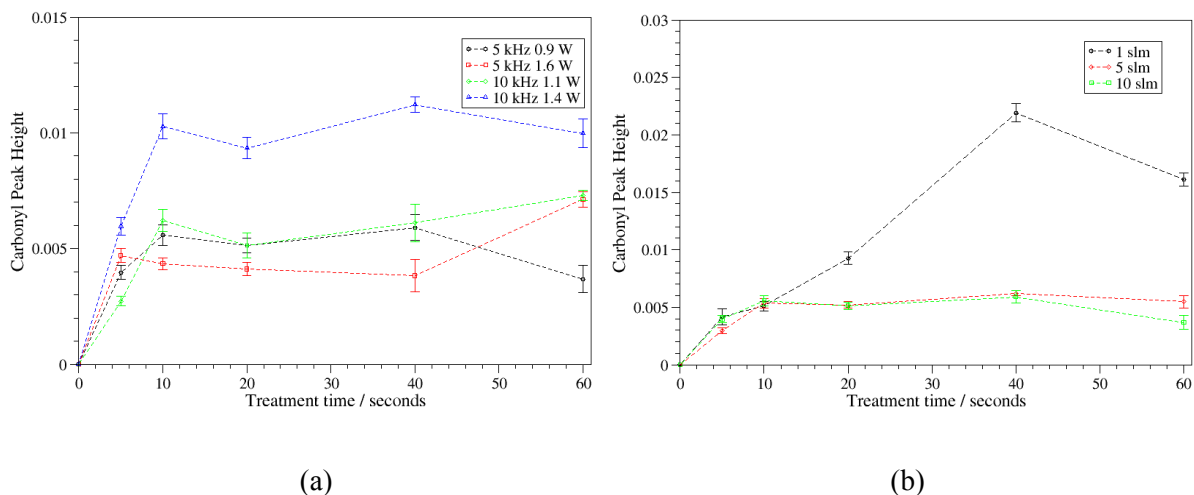


Figure 2: Peak height at  $1660\text{ cm}^{-1}$ , corresponding to maxima of carbonyl peak coming up with increased plasma treatment at different (a) powers and frequencies (nitrogen flow rate 5 slm), and (b) flow rates of nitrogen (frequency 5 kHz, power 1.1 W).

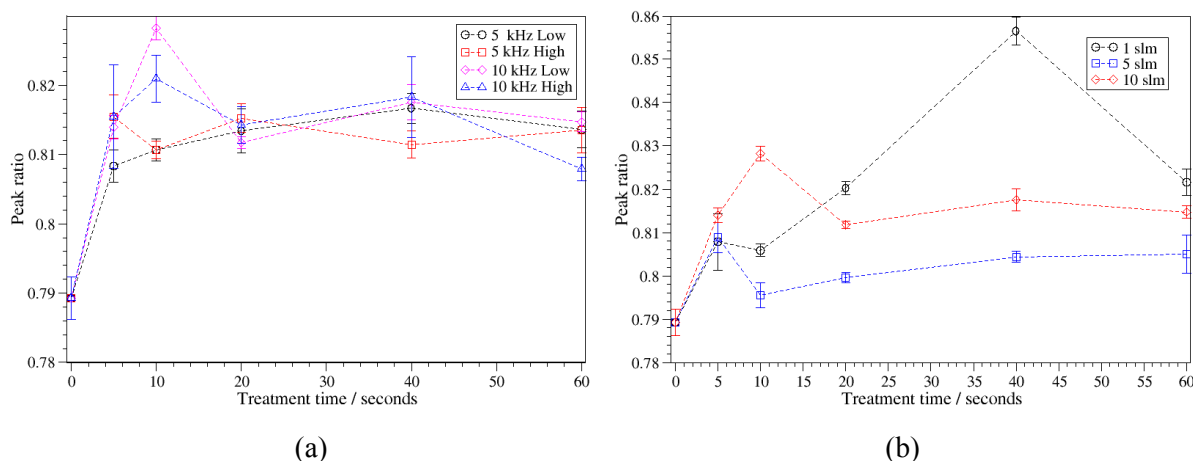
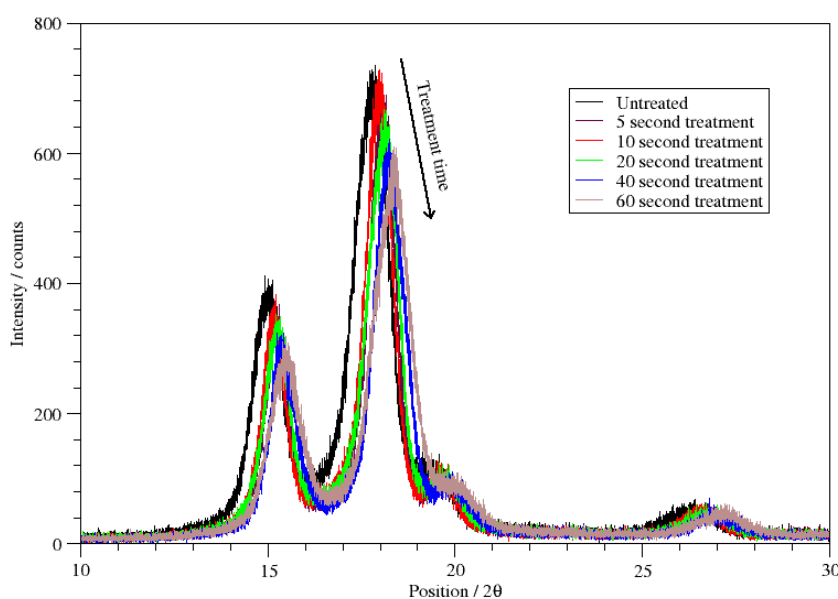


Figure 3: Peak ratios at  $997\text{ cm}^{-1}$  and  $973\text{ cm}^{-1}$  with processing time, indicating changes in crystallinity of the sample with plasma modification at different (a) powers and frequencies (nitrogen flow rate 5 slm), and (b) flow rates of nitrogen (frequency 5 kHz, power 1.1 W).

The BOPP films themselves tend to be highly crystalline, made up of interlocking lamella approximately 5 nm in diameter, with amorphous polypropylene chains linking the overall structure.<sup>[17]</sup> The amorphous regions are porous to gas,<sup>[18]</sup> and so will tend to retain oxygen as they are stored in ambient air prior to treatment by atmospheric pressure plasmas.<sup>[19]</sup> When exposed to the plasma, oxygen and nitrogen within these amorphous regions will react within the polymer surface, acting as a localised oxidising mechanism reacting with polypropylene

within these amorphous regions, whilst leaving oxidised functional groups in recessed crevices.

It perhaps indicates why there is also a plateau in Figure 2a and 2b, as the amorphous regions react rapidly, leaving the outer surfaces of the lamellae to react more slowly, reducing the rate of formation of carbonyl and amide groups vastly. Although the adsorbed oxygen is likely to be rapidly used up in the initial scission process within the amorphous regions, previous work by the authors has shown that trace amounts of oxygen present in the gas from possible leaks or impurities in the gas will form reactive oxygen species,<sup>[20]</sup> which will react with the surface of the BOPP film and provide the source of oxygen for the functional groups on the surface.



*Figure 4:* XRD patterns recorded for BOPP films at increasing plasma treatment times at a power of 0.9 W, frequency of 5 kHz and flow rate of 10 slm.

The changes in the crystal structure of the BOPP films are also shown in the XRD patterns displayed in **Figure 4**. The diffraction pattern shows the polypropylene film to be in the  $\beta$  form<sup>[21]</sup>. Figure 4 also demonstrates that the position of the XRD peaks show an increase in angular position with treatment time, indicating a definite reduction in d-spacing. This would

suggest that the crystalline lamella are relaxing into the space that is left as the amorphous regions within the BOPP film is preferentially oxidised.

The optical profilometry measurements show limited surface topology changes for most conditions studied, down to flow rates of 1 slm, at which point the roughness increases markedly at a higher power, **Figure 5** demonstrates this for selected conditions. This is believed to be due to the deposited energy density increasing in combination with a drop in flow rate, leading to more active species production producing more oxidation and scission of the BOPP. The roughened nature of the surface after treatment in this regime can be seen in Figure 5b and how the roughness at these conditions changes with respect to time can be seen in **Figure 6**. The linear increase in the roughness seen in Figure 6 would imply that there is greater oxidation of the surface due to the increased concentration of atomic oxygen within the plasma at these conditions. There is also potentially greater back diffusion of ambient air into the plasma at this lower flow rate.

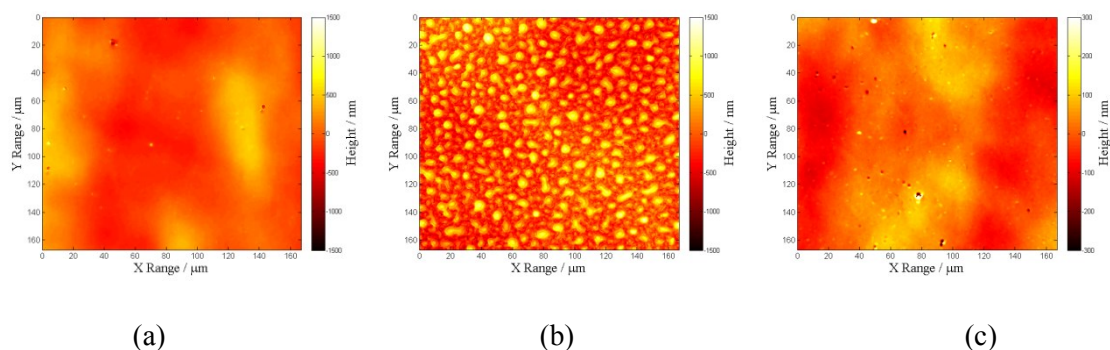


*Figure 5: Optical surface profilometry of (a) untreated BOPP film, (b) nitrogen plasma treated BOPP film, nitrogen flow rate 1 slm, treatment time 1 minute, (c) nitrogen plasma treated BOPP film, nitrogen flow rate 5 slm, treatment time 1 minute.*

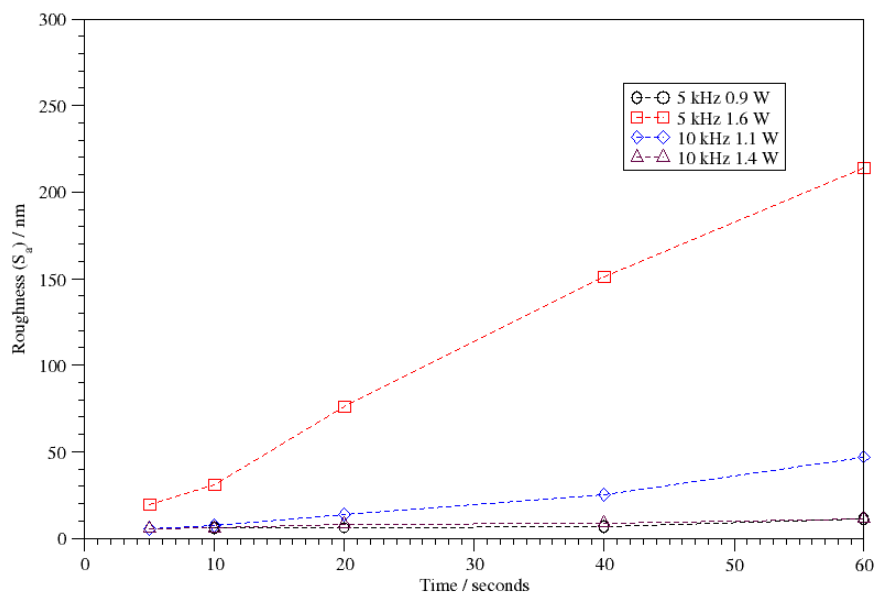
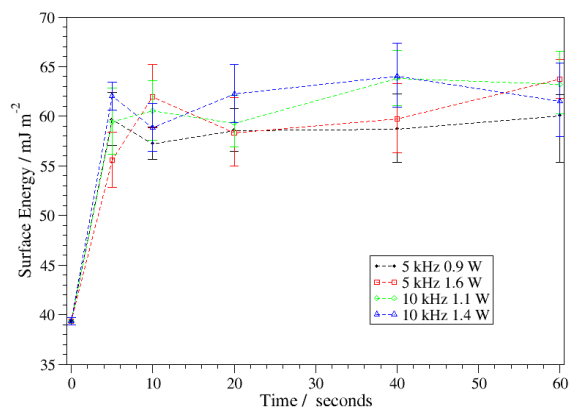
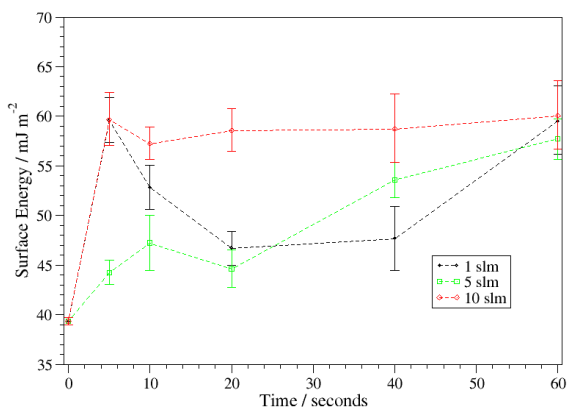


*Figure 6:* Roughness values measured for BOPP films at increasing plasma treatment times, flow rate 1 slm

Surface energy results for different flow-rates, powers and driving frequencies are presented in **Figure 7**. The surface energy increases with treatment time, with the polar component tending to increase while the dispersive component remains constant. Higher power to the plasma also marginally increases the surface energy, with frequency also displaying a slight effect. The same plateau as seen in Figure 3b and Figure 2a can be seen in Figure 7a, again implying that the crystal structure of the BOPP film is the controlling factor in an increase in functional groups with plasma treatment, and hence any surface energy increase. The surface energy at differing nitrogen flow rates are displayed in Figure 7b. Contact angles were also measured up to a fortnight after treatments were made, but no significant changes were measured.



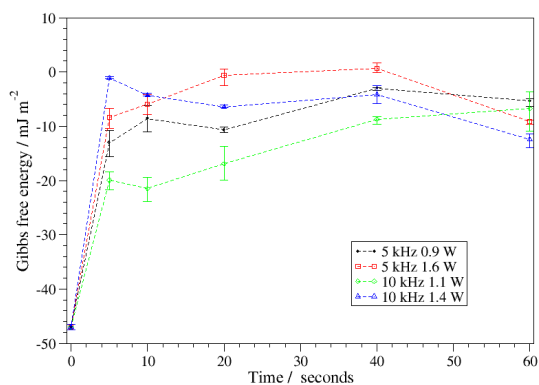
(a)



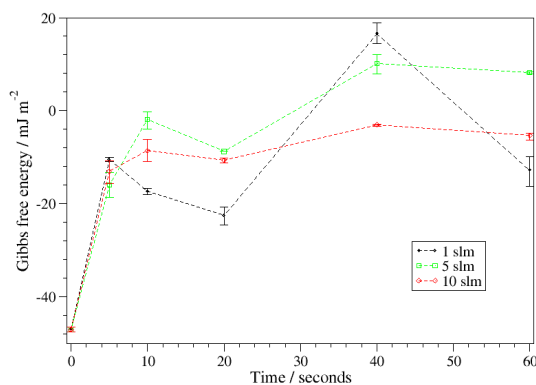
(b)

Figure 7: Surface energy with time at different (a) powers and frequencies (nitrogen flow rate 5 slm), and (b) different flow rates (frequency 5 kHz, power 1.1 W)

Figure 8 shows the increase in Gibbs Free Energy with plasma treatment exhibited under all conditions, showing an increase in the hydrophilic nature of the surface of the BOPP films after plasma treatment. The plateau with treatment time can again be seen in figure 8a, showing an effective maximum dependant on the crystalline structure of the BOPP film.



(a)



(b)

Figure 8: Gibbs free energy with time at different (a) powers and frequencies (nitrogen flow rate 5 slm), and (b) different flow rates (frequency 5 kHz, power 1.1 W)

## **4 Conclusion**

After a comprehensive study of the modification of BOPP films by nitrogen DBDs, it is evident that the crystal structure of the film itself is a key parameter in improving the surface functionality of BOPP films. The changes in the chemistry, crystal structure and topology of the BOPP surface have been studied with regards to the plasma process parameters, and the effects of the changes are not overwhelmingly strong on the overall increase in surface energy of the film. However, there is a plateau seen in the number of functional groups formed on the surface, and a plateau of the change in crystal structure, that corresponds with a plateau in the surface energy at about  $60 \text{ mJ m}^{-2}$ . This may imply the crystal structure of the film is the limiting factor for the increase of surface energy, and hence adhesion. Attempts to overcome this by increasing the effective energy density of the plasma start to cause intensive oxidation and scission of the BOPP as can be seen in Figure 5 and 6 when the flow rate is dropped and power increased, which roughens the surface of the film greatly, having implications for the optical properties. The treatments were carried out in the filamentary regime, and this has seemed to have shown no issues in terms of consistency of the treatment.

## **Acknowledgements**

The authors wish to thank the EPSRC project, “Ambient Processing of Polymeric Web: Advanced Diagnostics and Applications”, for the funding, Innovia Films for material and technical support, Lee Harman for technical support and Michael John Lynch for engineering design support.

## References

- [1] E. Liston, L. Martinu, and M. Wertheimer, *J. Adhes. Sci. Technol.*, **1993**, 7, 1091.
- [2] R. Dorai and M. J. Kushner, *J. Phys. D Appl. Phys.*, **2003**, 36, 666.
- [3] Et Es-sebbar, N. Gherardi and F. Massines, *J. Phy. D Appl. Phys.*, **2013**, 46.
- [4] D. Shaw, A. West, J. Bredin and E. Wagenaars, *Plasma Sources Sci. Technol.*, **2016**, 25.
- [5] L. F. MacManus, M. J. Walzak, and N. S. McIntyre, *J. Polym. Sci. Pol. Chem.*, **1999**, 37, 2489.
- [6] S. Guimond, I. Radu, G. Czeremuszkina, D. J. Carlsson, and M. R. Wertheimer, *Plasmas and Polymers*, **2002**, 7, 71.
- [7] J. Niu, D. Liu, and Y. Wu, *Surf. Coat. Tech.*, **2011**, 205, 3434.
- [8] S. Guimond and M. R. Wertheimer, *J. Appl. Polym. Sci.*, **2004**, 94, 1291.
- [9] K. Kostov, T. Nishime, L. Hein, and A. Toth, *Surf. Coat. Tech.*, **2013**, 234, 60.
- [10] A. Chiper and G. Borcia, *Plasma Chem. Plasma P.*, **2013**, 33, 553.
- [11] N. Naudé, J.-P. Cambronne, N. Gherardi, and F. Massines, *J. Phys. D Appl. Phys.*, **2005**, 38, 530.
- [12] R. Brandenburg, V. A. Maiorov, Y. B. Golubovskii, H.-E. Wagner, J. Behnke, and J. F. Behnke, *J. Phys. D Appl. Phys.*, **2005**, 38, 2187.
- [13] R. G. Quynn, J. L. Riley, D. A. Young, and H. D. Noether, *J. Appl. Polym. Sci.*, **1959**, 2, 166.

- [14] C. J. Van Oss, M. K. Chaudhury, R. J. Good, C. J. V. a. N. Oss, R. J. Good, C. J. Van Oss, and M. K. Chaudhury, *Chem. Rev.*, **1988**, *88*, 927.
- [15] C. J. Van Oss and R. F. Giese, *Clay. Clay Miner.*, **1995**, *43*, 474.
- [16] G. Socrates, *Infrared Characteristic Group Frequencies: Tables and Charts*. John Wiley and Sons, **1994**.
- [17] Y. Lin, P. Dias, H. Chen, A. Hiltner, and E. Baer, *Polymer*, **2008**, *49*, 2578.
- [18] S. G. Kiryushkin and Yu. A. Shlyapnikov, *Polym. Degrad. Stab.* **1989**, *23*, 185
- [19] W. L. Hawkins, W. Matreyek, and F. H. Winslow, *J. Polym. Sci.*, **1959**, *41*, 1.
- [20] Z. Abd-Allah, D. A. G. Sawtell, G. T. West, P. J. Kelly, and J. W. Bradley, *Plasma Process. Polym.*, **2016**, *13*, 649.
- [21] A. T. Jones, J. M. Aizlewood, and D. R. Beckett, *Makromol. Chem.*, **1964**, *75*, 134.